NeuroImage xxx (2013) xxx–xxx

Contents lists available at SciVerse ScienceDirect

NeuroImage

journal homepage: www.elsevier.com/locate/ynimg

Review

Differentiating functions of the lateral and medial prefrontal cortex in motor response inhibition

Achala H. Rodrigo [a], Stefano I. Di Domenico [a], Hasan Ayaz [b], Sean Gulrajani [a], Jaeger Lam [a], Anthony C. Ruocco [a,*]

[a] Department of Psychology, University of Toronto Scarborough, Toronto, Canada
[b] School of Biomedical Engineering, Science and Health Systems, Drexel University, Philadelphia, USA

ARTICLE INFO

Article history:
Accepted 25 January 2013
Available online xxxx

Keywords:
Near-infrared spectroscopy
Optical imaging
Response inhibition
Manual response control
Prefrontal cortex
Inferior frontal gyrus

ABSTRACT

The right inferior frontal gyrus is generally considered a critical region for motor response inhibition. Recent studies, however, suggest that the role of this cortical area in response inhibition may be overstated and that the contributions of other aspects of the prefrontal cortex are often overlooked. The current study used optical imaging to identify regions of the prefrontal cortex beyond the right inferior frontal gyrus which may serve to support motor response inhibition. Forty-three right-handed healthy adults completed a manual Go/No-Go task while evoked oxygenation of the prefrontal cortex was measured using 16-channel functional near-infrared spectroscopy. During motor response inhibition, the right inferior frontal gyrus, and to a lesser extent the homologous contralateral region, showed increased activation relative to a baseline task. Conversely, the medial prefrontal cortex was significantly deactivated, and the extent of reduced activity in this region was associated with fewer errors on the response inhibition task. These findings suggest a more substantial role of the left inferior frontal gyrus in response inhibition and possibly a distinct function of the middle frontal gyrus subserving error detection on manual motor control tasks.

Contents

* Corresponding author at: Department of Psychology, University of Toronto Scarborough, Toronto, Ontario, Canada M1C 1A4. Fax: +1 416 287 7642.
E-mail address: anthony.ruocco@gmail.com (A.C. Ruocco).

1053-8119/$ – see front matter © 2013 Elsevier Inc. All rights reserved.
http://dx.doi.org/10.1016/j.neuroimage.2013.01.059

Introduction

The prefrontal cortex (PFC) is a complex brain region that is thought to subserve a number of higher-order cognitive abilities (Miller and Cohen, 2001). Response inhibition represents perhaps one of the most extensively studied of these abilities, particularly with respect to motor control. The Go/No-Go paradigm has frequently been used to measure motor response inhibition across a variety of response modalities, including the hand, eye, and foot (Van't Ent and Apkarian, 1999). In general, this paradigm asks respondents to provide a specific motor response to a target stimulus (termed the *Go* stimulus) but to withhold this response to a non-target stimulus (known as the No-Go stimulus). Regardless of response modality, the Go/No-Go paradigm has been found to reliably activate the right inferior frontal gyrus (right IFG) under conditions of motor response inhibition (Chikazoe et al., 2007). Accordingly, Aron et al. (2004) concluded that this region, in coordination with the basal ganglia and perhaps other subcortical regions, is critical to response inhibition based on their analysis of neuroimaging and human lesion-mapping studies.

A recent meta-analysis of functional neuroimaging studies, however, suggests a different perspective on the prominence of the right IFG in response inhibition. Swick et al. (2011) examined 47 neuroimaging studies that employed a Go/No-Go paradigm and quantitatively synthesized their results using an activation-likelihood-estimation approach. This study revealed significant areas of right-hemisphere activation extending from the right IFG and middle frontal gyrus to the insular cortex and inferior parietal lobule. Significant foci of activation were also identified in the left superior, middle, and inferior frontal gyri. Therefore, in contrast to the widely reported finding of primarily right IFG activation on the Go/No-Go task, the anticipated dominance of this region in supporting response inhibition was not strongly implicated in this meta-analytic review. Notable limitations of this meta-analysis, however, were there it included a variety of Go/No-Go tasks which varied in their relative proportions of Go versus No-Go stimuli, which could impact the relative potency of a motor response and its associated functional activation (Nieuwenhuis et al., 2003). Also, given that most studies included in this meta-analysis comprised functional magnetic resonance imaging (fMRI) contrasts of a condition requiring a motor response (Go) with one that does not (No-Go), it is difficult to disentangle those areas of PFC activation related to the execution of a motor response (e.g., manually pressing a button on a Go trial) versus response inhibition (e.g., withholding a manual button press on a No-Go trial) when these two specific conditions are contrasted (Hester et al., 2004b).

Although fMRI has been used most frequently in prior studies of response inhibition, investigations based on other neuroimaging modalities may help to elucidate the relative contributions of distinct regions of the PFC to motor response inhibition. Functional near-infrared spectroscopy (fNIRS) is an optical brain imaging technique which measures relative changes in the concentrations of oxygenated (oxy-Hb) and deoxygenated hemoglobin (deoxy-Hb) based on the differential absorption and backscattering of infrared light in cortical tissue (for a review, see Irani et al., 2007). An important advantage of using fNIRS to advance our understanding of the role of the PFC in response inhibition is that it can generate distinct biological measures of cortical activation (i.e., oxy- and deoxy-Hb) which may convey information unique to that provided by the fMRI blood-oxygen level dependent signal (Steinbrink et al., 2006; Strangman et al., 2002). Importantly, fNIRS can supply these measures of cortical activation with high levels of temporal and spatial precision within the PFC, which may be crucial for unravelling the complexities of how functioning of this region may support response inhibition.

Only a small number of studies have employed fNIRS to investigate activation of the PFC under conditions of response inhibition using Go/No-Go tasks. These studies have revealed bilateral activation in the most anterior aspect of the IFG bilaterally (Herrmann et al., 2005), but also more dominant right IFG activation (Tsujii et al., 2011) during response inhibition. Similarly, Nishimura et al. (2011) detected significant activation within the left anterior IFG associated with response inhibition as well as an area of deactivation within the medial PFC (a finding which was not observed in a schizophrenia comparison group). Recently, Wriessnegger et al. (2012) used fNIRS to measure activation of the medial PFC and sensorimotor areas for 11 participants who completed finger and foot versions of a Go/No-Go task. They found significant activation of the medial PFC as well as deactivation of the corresponding sensorimotor cortex during motor response inhibition. Taken together, these findings suggest that activation of the homologous left IFG may also support response inhibition, whereas deactivation of specific prefrontal and sensorimotor cortical regions may also be implicated in some as yet unknown manner.

Although previous research using fNIRS to study response inhibition has revealed meaningful information about the potential roles of the left IFG and medial PFC in these processes, this research is limited in a number of ways. First, these investigations tended to utilize very brief activation periods (and sometimes only one activation period per condition) for their response inhibition tasks, thereby limiting the statistical power of these research designs. Second, nearly all prior fNIRS studies on this topic used probes that were limited in their spatial extent, and therefore, only one study simultaneously measured activation within medial and lateral portions of the PFC (including the IFG) (Nishimura et al., 2011). Given preliminary evidence from separate studies showing increased bilateral IFG activity in conjunction with reduced medial PFC activity during motor response inhibition, understanding the relative engagement and disengagement of these regions in a single study is potentially important. Third, the majority of this fNIRS research is based on considerably small samples of adults, limiting the extent to which meaningful conclusions can be drawn from any single study. Fourth, little research has examined the relationship between accuracy on response inhibition tasks and the extent of activation in specific neural regions. For example, research suggests that deactivation in midline areas (insula, medial PFC) prior to the inhibition of a motor response may be predictive of subsequent success in withholding that response (Hester et al., 2004b). Investigating the interaction between performance accuracy and cortical activation may elucidate whether discrete areas of the PFC function to support distinct response inhibition processes.

The present study accordingly set out to investigate several important unanswered questions regarding the role of inferior-lateral and medial areas of the PFC in motor response inhibition. First, we examined whether the homologous region in the left IFG is also recruited for motor response inhibition, contrary to previous claims of predominantly right IFG involvement (Aron et al., 2004). Second, we investigated whether the medial PFC shows significant deactivation associated with motor response inhibition, a finding which has been reported in only a small number of studies (Nishimura et al., 2011; Wriessnegger et al., 2012). To understand the potential interaction between behavioral performance and cortical activation, we also explored the relationship between accuracy on the Go/No-Go task and activation within inferior-lateral and medial aspects of the PFC.

Material and Methods

Participants

Forty-four right-handed healthy adults participated in this study. Participants were recruited from the University of Toronto Scarborough undergraduate research participant pool and the surrounding community. From this original sample, one participant was excluded due to problems with fNIRS signal acquisition during the experiment. In total, fNIRS data for seven men and 36 women with a mean age of 24.8 years ($SD = 11.3$) were included in our analyses. All individuals

Please cite this article as: Rodrigo, A.H., Differentiating functions of the lateral and medial prefrontal cortex in motor response inhibition, NeuroImage (2013), http://dx.doi.org/10.1016/j.neuroimage.2013.01.059

provided written informed consent to participate in this study, which was approved by the Research Ethics Board at the University of Toronto.

Procedure

Prior to commencing the response inhibition task, participants completed a brief screening interview to collect demographic information and rule out the presence of any serious manual, ophthalmic, neurologic (i.e., seizure disorder, severe head injury) or psychiatric illnesses (i.e., psychosis). Following this interview, participants were seated in a dimly-lit room in front of a computer monitor and a keyboard. They were asked to sit comfortably and interact with the computer by only pressing a designated button with their right index finger. Prior to beginning each task, instructions were presented on the monitor and read aloud by the experimenter. Testing did not proceed until participants acknowledged that they understood all instructions completely. After finishing all procedures, participants were compensated for their time with course credit or at a rate of $10 per hour.

fNIRS Setup

After the participant's forehead was cleaned using an alcohol swab, the fNIRS probe was positioned over the forehead and secured at the back of the head using Velcro® straps. The fNIR Imager 1000® (fNIR Devices, Potomac, MD) is a continuous-wave fNIRS system described in previous studies conducted by our research group (see Ayaz et al., 2012; Ruocco et al., 2010). Two wavelengths of light (730 nm and 850 nm) were measured continuously at 500 ms intervals in 16 channels with 1.25 cm penetration. The probe was aligned with the electrode positions F7, F_{P1}, F_{P2} and F8 based on the international 10–20 EEG system (Jasper, 1958), which corresponds to Brodmann areas 9, 10, 45 and 46. Specific details regarding probe placement are provided in Ayaz et al. (2011). Image reconstruction was rendered using the topographic tools available in fNIRSoft® Professional Edition (Ayaz, 2010) which provides spatial visualization of fNIRS activation data using MRI templates as described in Ayaz et al. (2006).

Measures

Scarborough Non-Affective Go/No-go Task (SNAG)

Participants completed a standard perceptual (non-affective) Go/No-Go task as part of a block-design paradigm which required them to press a button with their right index finger to Go stimuli (i.e., a green circle) and withhold a response to No-Go stimuli (i.e., a red circle). Each stimulus was presented on a black background for 500 ms, and participants were given a window of 3000 ms from the onset of the stimulus to respond. In total, 90 target stimuli and 30 non-target stimuli were arranged in six separate blocks. These six blocks were categorized into two conditions with three blocks per condition. *Go* blocks contained 20 (100%) Go stimuli, whereas *No-Go* blocks consisted of a quasi-random combination of 10 (50%) Go and 10 (50%) No-Go stimuli per block. In total, the SNAG maintained a ratio of 75% Go and 25% No-Go trials. This relative proportion of Go and No-Go trials was selected to increase the prepotency of the specified manual response. The inter-stimulus interval was jittered at increments of 500 ms (ranging from 4000 to 6000 ms, with a mean of 5000 ms) to discourage anticipatory responding. This task was intentionally designed with relatively long inter-stimulus intervals to ensure high levels of accuracy such that successful response inhibition could be examined. For each participant, the task always began with a Go block with subsequent blocks alternating between Go and No-Go.

Prior to completing the task, participants read the following instructions with accompanying graphical examples of the Go and No-Go stimuli: *You are going to see either a green or a red circle appear on the screen. Press the spacebar as fast as you can when you see the green circle. Don't press for the red circle, only the green circle. When the circle disappears, a plus sign will appear on the screen. Stare at the plus sign until the next circle appears. Remember to press the spacebar as fast as you can only when you see the green circle without making any mistakes.* Thus, both speed and accuracy were emphasized on this task. Participants were given the opportunity to ask questions and proceeded only when they acknowledged that they fully understood the task instructions.

Conners' Continuous Performance Test-II

We administered an extensively validated computerized laboratory test of motor response inhibition, the Conners' Continuous Performance Test-II (CPT-II; Conners, 2000), as a cross-validation behavioral measure for the SNAG. This task presents participants with a series of uppercase letters on a computer monitor and respondents are instructed to press the space bar for every letter, except for the letter *X*, and to do so as quickly and accurately as possible. The primary measure of motor response inhibition on the CPT-II is the number of commission errors on this task (i.e., incorrectly pressing the space bar for the letter *X*).

Signal Processing and Statistical Analysis

Raw fNIRS light intensities were manually screened and then underwent signal processing to exclude physiological artifacts using a low-pass filter with a finite impulse response and a linear phase filter with an order of 20 and a cut-off frequency of 0.1 Hz (Ayaz et al., 2010, 2012; Izzetoglu et al., 2004). Following these procedures, channels that showed signs of saturation or that were identified using a sliding-window motion artifact rejection (SMAR) technique (Ayaz et al., 2010) were identified and confirmed through visual inspection. On average, 2–3 channels were excluded for each participant primarily because of saturation with ambient light when contact with the skin was not optimal or in lateral channels due to interference from hair shafts. Time synchronization markers denoting the beginning and end of each block were delivered to the fNIRS acquisition device using a serial connection. Based on the markers that separated each activation block, data for local baseline segments and activation segments were extracted and compared.

Relative changes in oxy-Hb and deoxy-Hb for each activation condition were calculated relative to distinct local baselines for each condition. Each local baseline consisted of a 10-second cross-hair fixation period which immediately preceded each respective block. These local baselines were then aggregated to produce a baseline for comparison with Go and No-Go task conditions. Relative changes in oxy-Hb and deoxy-Hb for the two activation conditions were calculated relative to this baseline condition.

Data Analytic Approach

The fNIRS time-series data were analyzed with multilevel models (Bryk and Raudenbush, 1992; Kenny et al., 1998). Within the context of the present study, multilevel models take into account that the experimental time-series are nested within participants and that the number of observations may be unbalanced across participants. Variance in the dependent variable is partitioned into within-person (Level 1) and between-person (Level 2) components, allowing predictor terms to be represented at both the level of the experimental observation (Level 1) and at the level of the participant (Level 2). In the primary, whole-probe analyses, we examined the Level 1 effect of motor response inhibition. Type I error rate was controlled using the False Discovery Rate (Benjamini and Hochberg, 1995; Benjamini et al., 2001) to correct for multiple comparisons. In the secondary, region-of-interest (ROI) analyses, we examined the Level 1 effect of motor response inhibition, the Level 2 effect of behavioral accuracy (i.e., true negative responses on the SNAG), and the Motor Response Inhibition × Behavioral Accuracy cross-level interaction on participants' relative levels oxy-Hb in inferior-lateral and medial aspects of the PFC during the SNAG.

Please cite this article as: Rodrigo, A.H., Differentiating functions of the lateral and medial prefrontal cortex in motor response inhibition, NeuroImage (2013), http://dx.doi.org/10.1016/j.neuroimage.2013.01.059

The multilevel models were estimated in R (R Development Core Team, 2010) using the multilevel and nlme packages (Bliese, 2009). We estimated random intercept models, nesting the experimentally demarcated time-series data within each participant. To account for the temporal autocorrelation in the time-series, all models were conservatively estimated using an unstructured covariance matrix and the "between-within" method of estimating degrees of freedom (Schluchter and Elashoff, 1990).

Following the recommendations of West et al. (1996), we performed two sets of orthogonal contrasts to examine our *a priori* comparisons of interest. Of principle interest were the contrasts that examined the unstandardized mean differences in oxy-Hb between (a) the No-Go condition and its local baseline, (b) the Go condition and its local baseline, and (c) the Go and No-Go conditions. The first set of contrasts featured a term specifying the No-Go condition as "1/2" and its local baseline as "−1/2" while the Go condition and its local baseline were both coded as "0"; independent of this comparison, this contrast set also featured a term specifying the Go condition as "1/2" and its local baseline as "−1/2" while the No-Go condition and its local baseline were both coded as "0." The second set of contrasts featured a term specifying the Go condition as "1/2" and the No-Go condition as "−1/2" while the local baselines for both Go and No-Go were coded as "0." Thus, with respect to our measures of effect size and standard error, a one-unit difference on each contrast term represents the mean difference in oxy- and deoxy-Hb between our conditions of interest. For clarity of presentation, we strictly report the results of the above contrasts for oxy-Hb. It should be noted, however, that the estimated models featured code variables to comprehensively represent the overall treatment effect (West et al., 1996).[1] While we briefly summarize the results for deoxy-Hb, the complete analyses for this fNIRS parameter are available in the appended Supplementary Materials.

Results

Behavioral

High levels of accuracy were achieved on the SNAG with regard to true negative responses (i.e., correctly withholding responses to No-Go stimuli), $M = 93.7\%$, $SD = 6.09$, and true positive responses (i.e., correctly responding to Go stimuli), $M = 99.9\%$, $SD = 0.36$, with a mean reaction time (RT) of 344.6 ms ($SD = 54.9$). As expected, commission errors on the SNAG were significantly correlated with the same index on the CPT-II, $r\ (41) = 0.32$, $p = 0.04$, supporting the SNAG as a measure of motor response inhibition. Mean RT for commission errors on the SNAG ($M = 343.5$, $SD = 65.5$) was significantly faster ($M = 376.0$, $SD = 60.7$) than true positive responses, $t(29) = 2.70$, $p = 0.01$, suggesting that the few commissions on the SNAG represent genuine response inhibition errors (i.e., they are faster than correct responses on this task and could be considered more impulsive).

fNIRS

As detailed in Table 1, the intraclass correlations across the fNIRS channels ranged from 0.05 to 0.10 indicating a small but significant degree of dependence among participants' nested observations and a substantial amount of within-person variation during the time-course of the SNAG, as expected. The channel-wise time-series for oxy-Hb and deoxy-Hb during the No-Go condition is depicted in Fig. 1.

Table 1
Descriptive statistics for oxy-Hb time-series across fNIRS channels.

fNIRS Channel	Intraclass correlation	*N*	*n*
1	0.09	33,904	25
2	0.09	53,142	40
3	0.08	52,082	38
4	0.08	41,046	31
5	0.06	53,554	39
6	0.07	42,149	32
7	0.05	51,736	39
8	0.07	35,492	27
9	0.06	45,089	34
10	0.07	42,162	32
11	0.09	51,443	38
12	0.07	47,876	37
13	0.07	49,257	36
14	0.08	48,048	37
15	0.07	35,213	27
16	0.10	55,069	42

Note: All intraclass correlations are significant at $p<0.0001$. N = total number of observations, aggregated across all participants; n = total number of participants with available data. The numbers of observations across fNIRS channels are unbalanced due to filtering.

No-Go Versus Baseline

Table 2 reports the results of multilevel analyses comparing oxy-Hb across the No-Go and baseline conditions. Significant increases in oxy-Hb compared to baseline were observed in two clusters encompassing the anterior aspects of the right (channels: 13, 14, and 16) and left middle/inferior frontal gyri (channels 2 and 4), and a discrete area of activation situated in one channel over the left superior frontal gyrus (channel 5). Conversely, significant decreases in oxy-Hb compared to baseline were observed in the right medial PFC (channels 9 and 10). These results are portrayed in Fig. 2a.

With regard to deoxy-Hb, similar increases were observed in the left PFC, and to a lesser extent, the right PFC (channels 2, 3, 4, 5, 7, 12, and 13). Significant decreases were also seen in five channels largely in the right PFC (channels 6, 9, 11, 16, 10). As previously noted, the results of these analyses are available in the Supplementary Materials.

Go Versus Baseline contrasts

Table 3 reports the results of multilevel analyses comparing oxy-Hb across the Go and baseline conditions. Remarkable increases in oxy-Hb relative to baseline were observed in a large cluster that included the left and right medial PFC (channels 4, 6, 7, 8, 9, 10, 11, 12, 14). Conversely, significant decreases in oxy-Hb as compared to baseline were observed in an area comprising the right middle/inferior frontal gyri (channels 13 15). These results are portrayed in Fig. 2b. Significant decreases in deoxy-Hb were observed across the anterior PFC for this contrast (see Supplementary Materials).

Go Versus No-Go contrasts

Table 4 reports the results of multilevel analyses comparing oxy-Hb across the No-Go and Go conditions. The comparison of Go and No-Go conditions for oxy-Hb revealed higher activation for No-Go in two lateral clusters encompassing the left and right middle/inferior frontal gyri (channels 2, 3, 4, 13, 14, 15, and 16). On the other hand, Go activation was significantly higher than No-Go in medial channels across both the left and right medial PFC (channels 5, 6, 7, 8, 9, 10, 11, and 12,). These results are portrayed in Fig. 2c.

Significantly higher levels of deoxy-Hb were observed for No-Go condition as compared to Go condition for channels spanning the

[1] The first set of contrasts described above additionally featured a term specifying both the No-Go condition and its local baseline as "−1/2" while both the Go condition and its local baseline were both coded as "1/2." The second set of contrasts described above also featured two additional but similarly irrelevant terms. One term specified both the Go and the No-Go condition as "1/2" while the corresponding local baselines were both coded as "−1/2." The other term specified both the local baseline for the Go condition as "1/2" and the local baseline for the No-Go condition as "−1/2" while both the Go and No-Go conditions were coded as "0." Because these contrasts are of neither *a priori* nor exploratory interest, we do not report the corresponding results.

Please cite this article as: Rodrigo, A.H., Differentiating functions of the lateral and medial prefrontal cortex in motor response inhibition, NeuroImage (2013), http://dx.doi.org/10.1016/j.neuroimage.2013.01.059

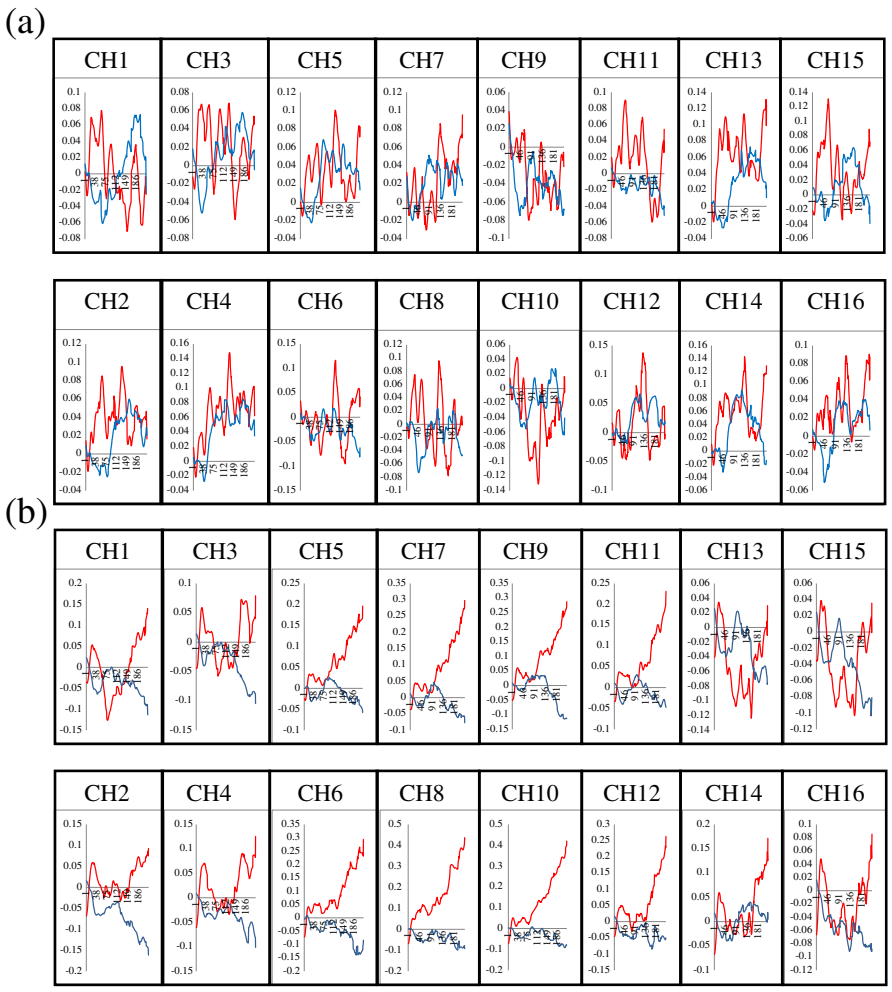

Fig. 1. Time-series of oxy-Hb and deoxy-Hb (μmolar) for all channels during No-Go (a) and Go (b) conditions.

anterior PFC bilaterally (channels 1, 2, 3, 4, 5, 6, 7, 8, 10, 12, 13, 14, 15, and 16). Conversely, lower levels of deoxy-Hb were detected in one channel corresponding to the right medial PFC (channel 9) for Go condition as compared to No-Go condition (see Supplementary Materials)

Table 2
Multilevel analyses comparing oxy-Hb levels across No-Go and baseline conditions.

fNIRS channel	*b*	*SE*	*df*	*T*
1	0.00	0.01	33,876	−0.23
2	0.04	0.01	53,099	3.62***
3	0.02	0.01	52,041	1.53
4	0.06	0.01	41,012	4.86***
5	0.03	0.01	53,512	3.24**
6	−0.01	0.01	42,114	−0.38
7	0.02	0.01	51,694	1.93†
8	0.00	0.02	35,462	0.28
9	−0.03	0.01	45,052	−2.48*
10	−0.04	0.01	42,127	−3.00**
11	0.01	0.01	51,402	1.35
12	0.02	0.01	47,836	1.18
13	0.07	0.01	49,218	5.63***
14	0.06	0.01	48,008	4.40***
15	0.03	0.02	35,183	1.99†
16	0.03	0.01	55,024	2.58*

Note: All models were estimated with an unstructured covariance matrix and the between-within method of estimating degrees of freedom. Significance levels are FDR corrected.
*** $p<0.001$.
** $p<0.01$.
* $p<0.05$.
† $p<0.10$.

Relationships Between Accuracy and PFC Activation

We estimated a set of nested multilevel models to examine the associations between performance on the Go/No-Go task and activation within areas of the inferior-lateral and medial PFC. Specifically, these models compared mean differences in oxy-Hb for our primary contrast of No-Go condition and its local baseline as a function of No-Go accuracy. The main effect for No-Go inhibition was entered at step 1. The main effect for No-Go accuracy was entered at step 2. The No-Go Inhibition × No-Go Accuracy cross-level interaction term was entered at step 3. Log-likelihood ratio tests were utilized to formally examine whether progressively complex models explained significantly greater amounts of variance in oxy-Hb (Snijders and Bosker, 1999). Separate models were estimated for specific ROIs, for which the respective observations were aggregated across a specific set of channels. The fNIRS channels featured different missing time-marked observations. Because these data were missing at random, the observed means for each ROI were calculated with listwise deletion. The right middle/IFG was defined by channels 13, 14, and 16; its corresponding models were estimated with 37,652 observations across 31 participants. The right medial PFC was defined by channels 9 and 10; its corresponding models were estimated with 33,926 observations across 27 participants. The left middle/IFG was defined by channels 2 and 4; its corresponding models were estimated with 39,787 observations across 31 participants. Finally, the left superior frontal gyrus was defined by the

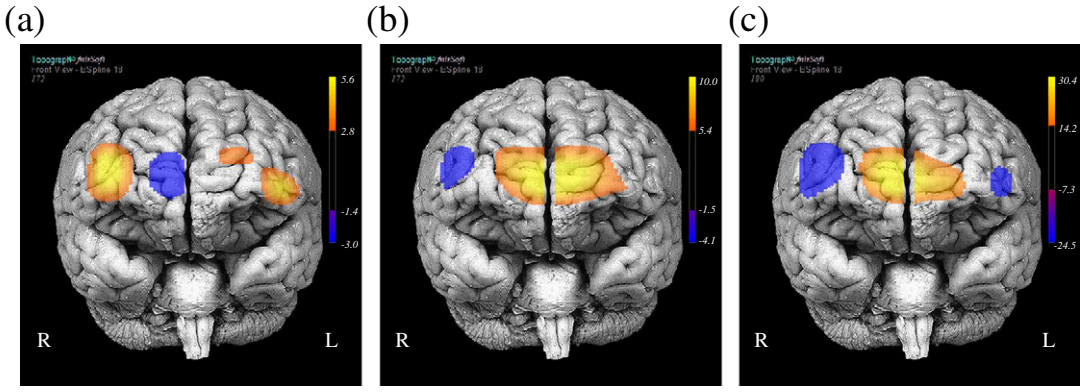

Fig. 2. Topographic images representing oxy-Hb for (a) No-Go−baseline, (b) Go−baseline, and (c) Go−No-Go activation contrasts. Images are overlaid onto an anatomical reference image of the brain. Values represent t-scores.

area activation observed in channel 5; its corresponding models were estimated using 53,554 observations across 39 participants. Table 5 displays the results of these multilevel analyses for the relevant predictors.

Right Lateral PFC. Although the log-likelihood ratio test indicated that the full model with interactions (step 3) explained significantly more variance than the simpler model (step 1 and 2), the No-Go Inhibition × No-Go Accuracy interaction was only marginally significant, $p = 0.0572$ (see Table 5). For exploratory purposes, we nonetheless plotted and examined the simple slopes of the No-Go Inhibition contrast term at high (+1 SD) and low (−1 SD) levels of No-Go accuracy (Aiken and West, 1991). The simple effect of No-Go inhibition was less pronounced and not significantly different than zero among participants achieving higher levels of No-Go Accuracy (+1 SD), $b = 0.03$, $SE = 0.02$, $t(37615) = 1.88$, $p = 0.0603$, relative to those participants with lower levels of No-Go Accuracy (−1 SD), for which the simple effect was significantly positive and greater than zero, $b = 0.08$, $SE = 0.02$, $t(37615) = 4.37$, $p < 0.0001$. These unstandardized regression coefficients signify that, in the right lateral PFC, No-Go inhibition predicted a 0.08 μmolar increase of oxy-Hb levels among those participants with lower levels of No-Go accuracy relative to baseline; among those participants with higher levels of No-Go Accuracy, No-Go inhibition did not predict any significant changes in oxy-Hb levels relative to baseline. Given that this interaction was only marginally significant, this trend should be interpreted with caution.

Right Medial PFC. For all remaining analyses (3.2.2.–3.2.2.4), the log-likelihood ratio test indicated that the full model with interactions (step 3) explained significantly more variance than the simpler model (steps 1 and 2). The No-Go Inhibition × No-Go Accuracy interaction for the right medial PFC was significant (see Table 5) and is illustrated in Fig. 3a. Following Aiken and West (1991), we plotted and examined the simple slopes of the No-Go Inhibition contrast term at high (+1 SD) and low (−1 SD) levels of No-Go accuracy. Interestingly, for participants with higher levels of No-Go accuracy (+1 SD), No-Go inhibition was associated with lower levels of oxy-Hb, $b = -.09$, $SE = 0.02$, $t(33893) = -4.46$, $p < 0.0001$, relative to those participants with lower levels of No-Go Accuracy (−1 SD), for which the simple effect was significantly positive, $b = 0.04$, $SE = 0.02$, $t(33893) = 2.17$, $p < 0.05$. To further investigate the significant No-Go Inhibition × No-Go Accuracy interaction term in the right medial PFC, we examined the simple slopes of No-Go accuracy at baseline and during No-Go inhibition. Although the simple effect of accuracy was not significant during baseline, higher levels of accuracy were associated with lower levels of oxy-Hb during No-Go inhibition, $b = -1.10$, $SE = 0.40$, $t(25) = -2.76$, $p < 0.05$. These results indicate that successful response inhibition was associated with significant deactivation in the right medial PFC during response inhibition.

Left Lateral PFC. The No-Go Inhibition × No-Go Accuracy interaction for the left lateral PFC was significant (see Table 5) and is illustrated in Fig. 3b. Examining the simple slopes of the No-Go Inhibition contrast

Table 3
Multilevel analyses comparing oxy-Hb levels across Go and baseline conditions.

fNIRS Channel	*b*	*SE*	*Df*	*t*
1	0.00	0.01	33,876	0.09
2	0.02	0.01	53,099	1.78†
3	0.01	0.01	52,041	0.82
4	0.03	0.01	41,012	1.94†
5	0.07	0.01	53,512	6.56**
6	0.09	0.01	42,114	6.43**
7	0.09	0.01	51,694	8.65**
8	0.17	0.02	35,462	9.97**
9	0.09	0.01	45,052	7.89**
10	0.14	0.01	42,127	9.67**
11	0.06	0.01	51,402	6.05**
12	0.06	0.01	47,836	4.53**
13	−0.05	0.01	49,218	−4.12**
14	0.03	0.01	48,008	2.40*
15	−0.07	0.01	35,183	−2.46*
16	−0.02	0.01	55,024	−1.50

Note: All models were estimated with an unstructured covariance matrix and the between-within method of estimating degrees of freedom. Significance levels are FDR corrected.
** $p < 0.001$.
* $p < 0.05$.
† $p < 0.10$.

Table 4
Multilevel analyses comparing oxy-Hb levels across Go and No-Go conditions.

fNIRS Channel	*b*	*SE*	*df*	*t*
1	−0.00	0.01	33,876†	−0.65
2	−0.03	0.00	53,099	−5.97**
3	−0.01	0.00	52,041	−3.28*
4	−0.05	0.01	41,012	−8.62**
5	0.03	0.00	53,512	7.24**
6	0.10	0.01	42,114	16.50**
7	0.07	0.00	51,694	15.97**
8	0.17	0.01	35,462	24.55**
9	0.13	0.00	45,052	25.41**
10	0.17	0.01	42,127	30.36**
11	0.04	0.00	51,402	10.02**
12	0.04	0.01	47,836	7.64**
13	−0.12	0.00	49,218	−24.51**
14	−0.04	0.00	48,008	−7.67**
15	−0.07	0.01	35,183	−11.98**
16	−0.06	0.00	55,024	−12.76**

Note: All models were estimated with an unstructured covariance matrix and the between-within method of estimating degrees of freedom. Significance levels are FDR corrected.
** $p < 0.001$.
* $p < 0.01$.

Please cite this article as: Rodrigo, A.H., Differentiating functions of the lateral and medial prefrontal cortex in motor response inhibition, NeuroImage (2013), http://dx.doi.org/10.1016/j.neuroimage.2013.01.059

Table 5
Multilevel models examining No-Go Accuracy across No-Go and baseline conditions.

ROI	Step	Predictor	*b*	*SE*	*df*	*t*	$\Delta\chi^2(df)$
Right Lateral PFC	Step 1	No-Go inhibition	0.05	0.01	37,618	4.20***	200.91(3)***
	Step 2	No-Go accuracy	0.38	0.43	29	0.87	.93(1)
	Step 3	No-Go inhibition × No-Go accuracy	−0.37	0.20	37,615	−1.90†	389.81(3)***
Right Medial PFC	Step 1	No-Go inhibition	−0.03	0.01	33,896	−2.02*	773.33(3)***
	Step 2	No-Go accuracy	−0.36	0.39	25	−0.92	.81(1)
	Step 3	No-Go inhibition × No-Go accuracy	−1.09	0.26	22,893	−4.23***	191.52(3)***
Left Lateral PFC	Step 1	No-Go inhibition	0.07	0.01	39,753	6.10***	147.62(3)***
	Step 2	No-Go accuracy	0.44	0.45	29	0.98	1.21(1)
	Step 3	No-Go inhibition × No-Go accuracy	−0.43	0.21	39,750	−2.02*	452.26(3)***
Left Superior Frontal Gyrus	Step 1	No-Go inhibition	0.03	0.01	53,512	3.24**	76.67(3)***
	Step 2	No-Go accuracy	−0.01	0.32	37	−0.03	.47(1)
	Step 3	No-Go inhibition × No-Go accuracy	−0.97	0.17	53,509	−5.77***	795.43(3)***

Note: All models were estimated with an unstructured covariance matrix and the between-within method of estimating degrees of freedom. The No-Go Inhibition term compared the unweighted mean of the No-Go condition with the corresponding local baseline condition. The No-Go Accuracy term was mean-centered. The log-likelihood ratio test at Step 1 compared the estimated model against an unconditional means model that specified an intercept with no predictors. The log-likelihood ratio test at Step 2 compared the previously estimated model at Step 1 against a model that additionally featured a main effect term for No-Go accuracy. Finally, the log-likelihood ratio test at Step 3 compared the previously estimated model at Step 2 against a model that additionally featured interactions for No-Go Accuracy and the three orthogonal contrast terms. PFC = prefrontal cortex.
*** $p<0.001$.
** $p<0.01$.
* $p<0.05$.
† $p<0.10$.

term at high (+1 SD) and low (−1 SD) levels of No-Go accuracy revealed that the simple effect of No-Go inhibition was weaker for participants with higher levels of No-Go accuracy (+1 SD), $b=0.05$, $SE=0.02$, $t(39750)=-3.11$, $p<0.01$, relative to those participants with lower levels of No-Go accuracy (−1 SD), $b=0.10$, $SE=0.02$, $t(39750)=5.48$, $p<0.0001$. The simple effect of No-Go accuracy was neither significant during baseline nor during No-Go inhibition. These results indicate that successful response inhibition was associated with significantly less activation in the left lateral PFC during response inhibition.

Left Superior Frontal Gyrus. The No-Go Inhibition × No-Go Accuracy interaction for the left superior frontal gyrus was significant (see Table 5). For participants with higher levels of No-Go accuracy (+1 SD), No-Go inhibition tended to be associated with decreased activation in the left superior frontal gyrus, $b=-.02$, $SE=0.01$, $t(53509)=-1.71$, $p=0.0865$. However, for participants with lower levels of No-Go Accuracy (−1 SD), the simple No-Go inhibition was associated with elevated hyper activation the left superior frontal gyrus, $b=0.09$, $SE=0.01$, $t(53509)=6.38$, $p<0.0001$. To further investigate this significant interaction, we examined the simple slopes of No-Go accuracy at during baseline and during No-Go inhibition. Although the simple effect of accuracy was not significant during baseline, higher levels of accuracy were associated with lower levels of oxy-Hb during No-Go inhibition, $b=-1.00$, $SE=0.32$, $t(37)=-3.06$, $p<0.01$. These results indicate that successful response inhibition is associated with significantly less activation in the left superior frontal gyrus during response inhibition.

Discussion

The current study evaluated manual motor response inhibition using a Go/No-Go task while activation in the PFC was monitored using 16-channel fNIRS. Analyses revealed higher levels of activity bilaterally in the middle/inferior frontal gyri as well as the left superior frontal gyrus under conditions of response inhibition. Conversely, significantly reduced activity was observed in the right medial PFC. Importantly, deactivation in this region during response inhibition was associated with greater accuracy on the Go/No-Go task. On the other hand, greater accuracy was associated with significantly less activation in the left lateral PFC during response inhibition. These findings suggest that the left inferior frontal gyrus may play a more prominent role in response inhibition than previously suggested while highlighting the potential importance of the middle frontal gyrus for the detection of errors on tests of manual motor control.

The right IFG has been strongly implicated in studies of response inhibition using diverse neuroimaging and lesion-mapping techniques (Aron et al., 2004). Consistent with our hypotheses, the present study provided additional support for these findings by demonstrating that conditions of response inhibition were associated with significant increases in activation within the right IFG. Recently, the distinct importance of this region in subserving response inhibition has been questioned in a meta-analytic review of fMRI studies investigating the neural correlates of this cognitive function (Swick et al., 2011). The suggestion was that right IFG activation may be an artifact of fMRI spatial

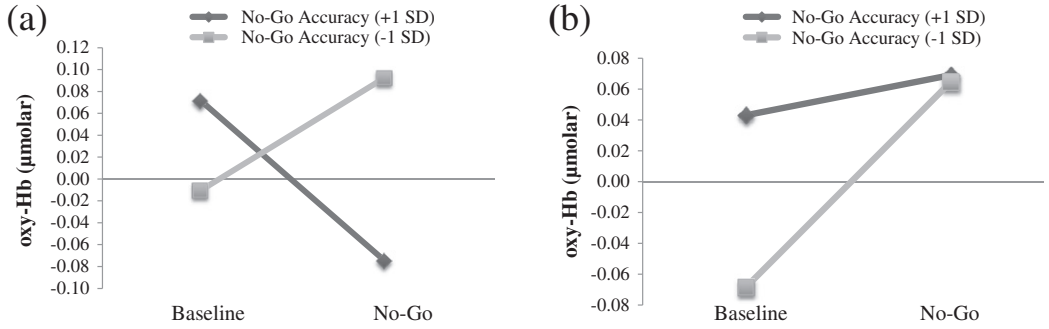

Fig. 3. Predicted levels of oxy-Hb in (a) right medial prefrontal cortex and (b) left lateral prefrontal cortex in µmoles for baseline and No-Go activation conditions. Note: SD = standard deviation.

Please cite this article as: Rodrigo, A.H., Differentiating functions of the lateral and medial prefrontal cortex in motor response inhibition, NeuroImage (2013), http://dx.doi.org/10.1016/j.neuroimage.2013.01.059

smoothing techniques which could inaccurately localize activity to this region when in fact it may originate from within the insular cortex. Importantly, our use of fNIRS in this study allowed us to measure cortical activity with a depth of penetration (1.25 cm) that is very unlikely to include activation within the insula. Additionally, no spatial smoothing procedures were applied to our data which could have obscured the spatial extent of the activations observed in this study. Therefore, these results derived from fNIRS based techniques lend support to the right IFG as a critical region subserving motor inhibitory processes.

There has also been an increasing acknowledgment that the left IFG may be activated along with the right IFG on tasks requiring motor response inhibition. Several such studies using fMRI, fNIRS, and lesion-mapping, have found that this homologous region within the left hemisphere may also be critical for response inhibition (Swick et al., 2008, 2011; Wriessnegger et al., 2012). Consistently, the present study observed significant increases in activation (No-Go −baseline) within three channels comprising the most anterior aspects of the middle and inferior frontal gyri in the left hemisphere. In contrast, activation within the right lateral region of the PFC was distributed over a larger area of the middle and inferior frontal gyri and extended from the most anterior portion of the PFC to the most dorsal region of the probe. These findings, therefore, are consistent with emerging research which suggests that both the right and left areas of the lateral PFC may be engaged for motor response inhibition, with the results of this study suggesting perhaps a greater extent of activation in the right lateral PFC.

Considering that significant increases in activation under conditions of response inhibition were observed within lateral regions of the PFC, it was perhaps surprising that highly accurate performances on the Go/No-Go task were associated with attenuated increases in activation within these regions bilaterally. Conversely, unlike their more accurate counterparts, participants who were less accurate appeared to show notable increases in oxy-Hb under conditions of response inhibition. These findings may be indicative of "neural efficiency" (for an example using fNIRS, see Leon-Carrion et al., 2010) among those who were very highly successful at inhibiting their motor responses, given that participants, on average, achieved high levels of accuracy on this task (~94% true negatives). In light of this consideration, we examined the number of commission errors made by participants in the highly accurate group and found that these individuals made no errors on the Go/No-Go task. These results could suggest that the lateral PFC may not only function to inhibit prepotent responses but also play a more complex role associated with error monitoring, a process invoked primarily in the presence of errors. This would be in line with previous findings demonstrating that lateral PFC, in conjunction with the anterior cingulate cortex, may guide error monitoring and other compensatory functions (Gehring and Knight, 2000). Further research using event-related designs and neuroimaging modalities allowing for a greater depth of penetration is needed to more fully investigate these speculations. Our findings, however, provide initial evidence ascribing a more complex function to the lateral PFC which goes beyond inhibitory processes to include error-monitoring, perhaps in combination with the anterior cingulate cortex.

In addition to recruitment of the lateral PFC, emerging research suggests that medial portions of the frontal cortex may actually show significant deactivation associated with motor response inhibition (Wriessnegger et al., 2012). Our findings were in line with these expectations, as they revealed robust deactivation of the right medial PFC under conditions of response inhibition. To investigate the functional significance of this deactivation, we conducted moderation analyses that examined whether and how different levels of accuracy on the Go/No-Go task (defined as true negative responses) predicted activity in the right medial PFC. These analyses indicated that individuals who reached the highest levels of accuracy on this task showed greater deactivation in the right medial PFC as compared to those who achieved lower levels of accuracy. Deactivation of this region has been demonstrated in previous fMRI work examining motor response inhibition (Hester et al., 2004b), showing that deactivation in the medial PFC may be associated with higher accuracy on response inhibition tasks. The proposal of these researchers was that while activation of task-relevant regions (i.e., lateral PFC) may favor successful response inhibition, failure to suppress task-irrelevant activation (i.e., medial PFC) may lead to interference with efficient task performance.

More speculatively, another (non-mutually exclusive) possibility concerns the role of the medial PFC in self-referential processes (Lieberman, 2007; Mitchell, 2009; Northoff and Bermpohl, 2004). A large number of imaging studies highlight the medial PFC in various forms of self-reflection such as reflecting upon one's own personality traits, feelings, and physical attributes (e.g., Jenkins and Mitchell, 2011). Interestingly, research from the field of motivation characterizes optimal performance along experiential lines as involving a transient "loss of self-consciousness" (Csikszentmihalyi, 1990; also see Deci et al., 1999). Similarly, developmental psychologists have long noted that one of the cardinal phenomenological features of successful self-control is cognitive automaticity or the relative absence of subjective "self-exertion" (e.g., see Pascual-Leone, 1990). The presently observed relationship between behavioral accuracy and medial PFC deactivation during the No-Go task is in correspondence with these ideas, suggesting that deactivation of this region in specific contexts may constitute an index of one's neural disposition for optimal task engagement (cf. Gusnard and Raichle, 2001; Sheline et al., 2009). Although the present research was not specifically designed, and therefore is not well-suited, to thoroughly examine this possibility, our results suggest that future research would benefit by investigating the functional role of task-induced medial PFC deactivations in the prediction of behavioral performance.

A number of limitations should be noted in reference to the results of this study. First, an important constraint of the fNIRS system employed in the present study was that it could not provide measurements of hemodynamic activity with acceptable levels of spatial precision in subcortical regions. Related, the probe used in this study provided coverage of the PFC bilaterally, which allowed us to advance prior fNIRS research by measuring medial and lateral regions simultaneously; however, we could not measure activation in more dorsal aspects of the frontal cortex which may play a role in motor response inhibition (Wriessnegger et al., 2012). Second, our use of a block-design precluded us from examining trial-wise activation associated with correct and incorrect responses, although there were very few of the latter. Therefore, an event-related design may also help to further differentiate functions of the medial and lateral regions of the PFC subserving specific aspects of response inhibition. Third, whereas this study represents one of the largest investigations ($N = 43$) of response inhibition using fNIRS, this sample of participants was composed primarily of females, and there is emerging research which suggests that there may be subtle sex differences in PFC activation associated with response inhibition (Garavan et al., 2006; Hester et al., 2004a; Li et al., 2006). Future work should strive to achieve greater balance in this respect, which might allow for investigation of potential sex differences in the neural systems underlying response inhibition.

In summary, the findings of the current study suggest that the middle and inferior frontal gyri may be bilaterally activated under conditions of motor response inhibition. Less activation within these regions, particularly on the left side, may be associated with a reduced likelihood of inhibitory errors. The medial PFC, on the other hand, showed significantly reduced activity during response inhibition, with fewer inhibitory errors associated with the extent of deactivation observed in this region. This pattern of findings suggests that the lateral and medial aspects of the PFC may support distinct functions as they relate to manual motor response control.

Please cite this article as: Rodrigo, A.H., Differentiating functions of the lateral and medial prefrontal cortex in motor response inhibition, NeuroImage (2013), http://dx.doi.org/10.1016/j.neuroimage.2013.01.059

Acknowledgements

We would like to thank Dr. Elizabeth Page-Gould for statistical consultation.

Appendix A. Supplementary data

Supplementary data to this article can be found online at http://dx.doi.org/10.1016/j.neuroimage.2013.01.059.

References

Aiken, L.S., West, S.G., 1991. Multiple Regression: Testing and Interpreting Interactions. Sage Publications, Incorporated.
Aron, A.R., Robbins, T.W., Poldrack, R.A., 2004. Inhibition and the right inferior frontal cortex. Trends Cogn. Sci. 8, 170–177.
Ayaz, H., 2010. Functional near infrared spectroscopy based brain computer interface. School of Biomedical Engineering Science & Health Systems. Drexel University, Philadelphia, PA, p. 214 (PhD Thesis).
Ayaz, H., Izzetoglu, M., Platek, S.M., Bunce, S., Izzetoglu, K., Pourrezaei, K., Onaral, B., 2006. Registering fNIR data to brain surface image using MRI templates. 2006 28th Annual International Conference of the IEEE Engineering in Medicine and Biology Society, vols. 1–15, pp. 4906–4909.
Ayaz, H., Izzetoglu, M., Shewokis, P.A., Onaral, B., 2010. Sliding-window motion artifact rejection for Functional Near-Infrared Spectroscopy. Conf. Proc. IEEE Eng. Med. Biol. Soc. 2010, 6567–6570.
Ayaz, H., Shewokis, P.A., Curtin, A., Izzetoglu, M., Izzetoglu, K., Onaral, B., 2011. Using MazeSuite and functional near infrared spectroscopy to study learning in spatial navigation. J. Vis. Exp. (56), e3443, http://dx.doi.org/10.3791/3443 (http://www.jove.com/video/3443/using-mazesuite-functional-near-infrared-spectroscopy-to-study?id=3443).
Ayaz, H., Shewokis, P.A., Bunce, S., Izzetoglu, K., Willems, B., Onaral, B., 2012. Optical brain monitoring for operator training and mental workload assessment. NeuroImage 59, 36–47.
Benjamini, Y., Hochberg, Y., 1995. Controlling the false discovery rate: a practical and powerful approach to multiple testing. J. R. Stat. Soc. Ser. B 57, 289–300.
Benjamini, Y., Drai, D., Elmer, G., Kafkafi, N., Golani, I., 2001. Controlling the false discovery rate in behavior genetics research. Behav. Brain Res. 125, 279–284.
Bliese, P., 2009. Multilevel Modeling in R (2.3): A brief introduction to R, the multilevel package and the nlme package.
Bryk, A.S., Raudenbush, S.W., 1992. Hierarchical linear models. Sage, Newbury Park, CA.
Chikazoe, J., Konishi, S., Asari, T., Jimura, K., Miyashita, Y., 2007. Activation of right inferior frontal gyrus during response inhibition across response modalities. J. Cogn. Neurosci. 19, 69–80.
Conners, C.K., 2000. Conners' Continuous Performance Test II: Computer Program for Windows Technical Guide and Software Manual. Mutli-Health Systems, Toronto, Canada.
Csikszentmihalyi, M., 1990. Flow. Harper & Row, New York, NY.
Deci, E.L., Koestner, R., Ryan, R.M., 1999. A meta-analytic review of experiments examining the effects of extrinsic rewards on intrinsic motivation. Psychol. Bull. 125, 627–668 (discussion 692–700).
Garavan, H., Hester, R., Murphy, K., Fassbender, C., Kelly, C., 2006. Individual differences in the functional neuroanatomy of inhibitory control. Brain Res. 1105, 130–142.
Gehring, W.J., Knight, R.T., 2000. Prefrontal-cingulate interactions in action monitoring. Nat. Neurosci. 3, 516–520.
Gusnard, D.A., Raichle, M.E., 2001. Searching for a baseline: Functional imaging and the resting human brain. Nat. Rev. Neurosci. 2, 685–694.
Herrmann, M.J., Plichta, M.M., Ehlis, A.C., Fallgatter, A.J., 2005. Optical topography during a Go-NoGo task assessed with multi-channel near-infrared spectroscopy. Behav. Brain Res. 160, 135–140.
Hester, R., Fassbender, C., Garavan, H., 2004a. Individual differences in error processing: a review and reanalysis of three event-related fMRI studies using the GO/NOGO task. Cereb. Cortex 14, 986–994.
Hester, R.L., Murphy, K., Foxe, J.J., Foxe, D.M., Javitt, D.C., Garavan, H., 2004b. Predicting success: patterns of cortical activation and deactivation prior to response inhibition. J. Cogn. Neurosci. 16, 776–785.
Irani, F., Platek, S.M., Bunce, S., Ruocco, A.C., Chute, D., 2007. Functional near infrared spectroscopy (fNIRS): an emerging neuroimaging technology with important applications for the study of brain disorders. Clin. Neuropsychol. 21, 9–37.
Izzetoglu, K., Bunce, S., Izzetoglu, M., Onaral, B., Pourrezaei, K., 2004. Functional near-infrared neuroimaging. Conf. Proc. IEEE Eng. Med. Biol. Soc. 7, 5333–5336.
Jasper, H.H., 1958. Report of the committee on methods of clinical examination in electroencephalography. Electroencephalogr. Clin. Neurophysiol. 370–375.
Jenkins, A.C., Mitchell, J.P., 2011. Medial prefrontal cortex subserves diverse forms of self-reflection. Soc. Neurosci. 6, 211–218.
Kenny, D.A., Kashy, D.A., Bolger, N., 1998. Data analysis in social psychology. McGraw-Hill, New York, NY.
Leon-Carrion, J., Izzetoglu, M., Izzetoglu, K., Martin-Rodriguez, J.F., Damas-Lopez, J., Barroso y Martin, J.M., Dominguez-Morales, M.R., 2010. Efficient learning produces spontaneous neural repetition suppression in prefrontal cortex. Behav. Brain Res. 208, 502–508.
Li, C.S., Huang, C., Constable, R.T., Sinha, R., 2006. Gender differences in the neural correlates of response inhibition during a stop signal task. NeuroImage 32, 1918–1929.
Lieberman, M.D., 2007. Social cognitive neuroscience: a review of core processes. Annu. Rev. Psychol. 58, 259–289.
Miller, E.K., Cohen, J.D., 2001. An integrative theory of prefrontal cortex function. Annu. Rev. Neurosci. 24, 167–202.
Mitchell, J.P., 2009. Social psychology as a natural kind. Trends Cogn. Sci. 13, 246–251.
Nieuwenhuis, S., Yeung, N., van den Wildenberg, W., Ridderinkhof, K.R., 2003. Electrophysiological correlates of anterior cingulate function in a go/no-go task: effects of response conflict and trial type frequency. Cogn. Affect. Behav. Neurosci. 3, 17–26.
Nishimura, Y., Takizawa, R., Muroi, M., Marumo, K., Kinou, M., Kasai, K., 2011. Prefrontal cortex activity during response inhibition associated with excitement symptoms in schizophrenia. Brain Res. 1370, 194–203.
Northoff, G., Bermpohl, F., 2004. Cortical midline structures and the self. Trends Cogn. Sci. 8, 102–107.
Pascual-Leone, J., 1990. An essay on wisdom: toward organismic processes that make it happen. In: Sternberg, R.J. (Ed.), Wisdom: Its Nature, Origins, and Development. Cambridge University Press, New York, NY, pp. 244–278.
R Development Core Team, 2010. R: a language and environment for statistical computing. Retrieved from http://www.lsw.uniheidelberg.de/users/christlieb/teaching/UKStaSS10/R-refman.pdf.
Ruocco, A.C., Medaglia, J.D., Ayaz, H., Chute, D.L., 2010. Abnormal prefrontal cortical response during affective processing in borderline personality disorder. Psychiatry Res. 182, 117–122.
Schluchter, M.D., Elashoff, J.T., 1990. Small-sample adjustments to tests with unbalanced repeated measures assuming several covariance structures. J. Stat. Comput. Simul. 37, 69–87.
Sheline, Y.I., Barch, D.M., Price, J.L., Rundle, M.M., Vaishnavi, S.N., Snyder, A.Z., Mintun, M.A., Wang, S., Coalson, R.S., Raichle, M.E., 2009. The default mode network and self-referential processes in depression. Proc. Natl. Acad. Sci. U. S. A. 106, 1942–1947.
Snijders, T.A.B., Bosker, R.J., 1999. Multilevel analysis: an introduction to basic and advanced multilevel modeling. Sage Publications, Incorporated.
Steinbrink, J., Villringer, A., Kempf, F., Haux, D., Boden, S., Obrig, H., 2006. Illuminating the BOLD signal: combined fMRI-fNIRS studies. Magn. Reson. Imaging 24, 495–505.
Strangman, G., Culver, J.P., Thompson, J.H., Boas, D.A., 2002. A quantitative comparison of simultaneous BOLD fMRI and NIRS recordings during functional brain activation. NeuroImage 17, 719–731.
Swick, D., Ashley, V., Turken, U., 2008. Left inferior frontal gyrus is critical for response inhibition. BMC Neurosci. 9.
Swick, D., Ashley, V., Turken, U., 2011. Are the neural correlates of stopping and not going identical? Quantitative meta-analysis of two response inhibition tasks. NeuroImage 56, 1655–1665.
Tsujii, T., Sakatani, K., Nakashima, E., Igarashi, T., Katayama, Y., 2011. Characterization of the acute effects of alcohol on asymmetry of inferior frontal cortex activity during a Go/No-Go task using functional near-infrared spectroscopy. Psychopharmacology 217, 595–603.
Van't Ent, D., Apkarian, P., 1999. Motoric response inhibition in finger movement and saccadic eye movement: a comparative study. Clin. Neurophysiol. 110, 1058–1072.
West, S.G., Aiken, L.S., Krull, J.L., 1996. Experimental personality designs: analyzing categorical by continuous variable interactions. J. Personal. 64, 1–48.
Wriessnegger, S.C., Bauernfeind, G., Schweitzer, K., Kober, S., Neuper, C., Muller-Putz, G.R., 2012. The interplay of prefrontal and sensorimotor cortices during inhibitory control of learned motor behavior. Front. Neuroeng. 5, 17.

Please cite this article as: Rodrigo, A.H., Differentiating functions of the lateral and medial prefrontal cortex in motor response inhibition, NeuroImage (2013), http://dx.doi.org/10.1016/j.neuroimage.2013.01.059